Journal of Computational Physics 351 (2017) 216–229

Contents lists available at ScienceDirect

Journal of Computational Physics

www.elsevier.com/locate/jcp

An energy-conserving method for stochastic Maxwell equations with multiplicative noise

Jialin Hong [a], Lihai Ji [b], Liying Zhang [c,*], Jiaxiang Cai [d]

[a] Institute of Computational Mathematics and Scientific/Engineering Computing, Academy of Mathematics and Systems Science, Chinese Academy of Sciences, Beijing 100190, China
[b] Institute of Applied Physics and Computational Mathematics, Beijing 100094, China
[c] School of Mathematical Science, China University of Mining and Technology, Beijing 100083, China
[d] School of Mathematical Science, Huaiyin Normal University, Huai'an, Jiangsu 210046, China

ARTICLE INFO

Article history:
Received 14 July 2016
Received in revised form 20 July 2017
Accepted 18 September 2017
Available online 21 September 2017

Keywords:
Energy-conserving method
Three-dimensional stochastic Maxwell equations
Multiplicative noise
Geometric structure

ABSTRACT

In this paper, it is shown that three-dimensional stochastic Maxwell equations with multiplicative noise are stochastic Hamiltonian partial differential equations possessing a geometric structure (i.e. stochastic multi-symplectic conservation law), and the energy of system is a conservative quantity almost surely. We propose a stochastic multi-symplectic energy-conserving method for the equations by using the wavelet collocation method in space and stochastic symplectic method in time. Numerical experiments are performed to verify the excellent abilities of the proposed method in providing accurate solution and preserving energy. The mean square convergence result of the method in temporal direction is tested numerically, and numerical comparisons with finite difference method are also investigated.

1. Introduction

In this paper, we consider three-dimensional (3D) stochastic Maxwell equations with multiplicative noise [18]

$$\begin{aligned} d\mathbf{E}(\mathbf{t},\mathbf{x},\mathbf{y},\mathbf{z}) &= \nabla\times\mathbf{H}(\mathbf{t},\mathbf{x},\mathbf{y},\mathbf{z})dt-\lambda\mathbf{H}(\mathbf{t},\mathbf{x},\mathbf{y},\mathbf{z})\circ dW(t),\\ d\mathbf{H}(\mathbf{t},\mathbf{x},\mathbf{y},\mathbf{z}) &= -\nabla\times\mathbf{E}(\mathbf{t},\mathbf{x},\mathbf{y},\mathbf{z})dt+\lambda\mathbf{E}(\mathbf{t},\mathbf{x},\mathbf{y},\mathbf{z})\circ dW(t), \end{aligned} \tag{1.1}$$

where $t\in[0,T]$, $(x,y,z)\in\Theta\subset\mathbb{R}^3$, and Θ is a bounded and simply connected domain with smooth boundary $\partial\Theta$. We employ the perfectly electric conducting (PEC) boundary condition

$$\mathbf{E}\times\mathbf{n}=\mathbf{0} \tag{1.2}$$

on $(0,T]\times\partial\Theta$, where $\mathbf{n}$ is the unit outward normal of $\partial\Theta$. The above system is understood in the Stratonovich setting and the symbol $\circ$ stands for the Stratonovich product. Here, $\lambda\geq 0$ measures the size of the noise and W is a Q-Wiener process defined on a given probability space $(\Omega,\mathscr{F},P,\{\mathscr{F}_t\}_{t\in[0,T]})$, with values in the Hilbert space $\mathbb{L}^2(\Theta)$, which is a space of square integrable real-valued functions. Let $\{e_m\}_{m\in\mathbb{N}}$ be an orthonormal basis of $\mathbb{L}^2(\Theta)$ consisting of eigenvectors of a symmetric, nonnegative and finite trace operator Q, i.e., $Tr(Q)=\sum\limits_{m\in\mathbb{N}}\langle Qe_m,e_m\rangle_{L_2}=\sum\limits_{m\in\mathbb{N}}\eta_m<\infty$

* Corresponding author.
E-mail addresses: hjl@lsec.cc.ac.cn (J. Hong), jilihai@lsec.cc.ac.cn (L. Ji), lyzhang@lsec.cc.ac.cn (L. Zhang), thomasjeer@sohu.com (J. Cai).

https://doi.org/10.1016/j.jcp.2017.09.030

and $Qe_m = \eta_m e_m$. Then there exists a sequence of independent real-valued Brownian motions $\{\beta_m\}_{m\in\mathbb{N}}$ such that $W(t,x,y,z,\omega) = \sum_{m=0}^{\infty} \sqrt{\eta_m}\beta_m(t,\omega)e_m(x,y,z), \quad t \geq 0, (x,y,z) \in \Theta, \omega \in \Omega$.

3D stochastic Maxwell equations with multiplicative noise play an important role in many scientific fields, especially in stochastic electromagnetism and statistical radiophysics [2,8,13,18]. We refer interested readers to [15] for the well-posedness of equations (1.1). By using infinite dimensional Itô formula, it is straightforward to show that the $L^2(\Theta)$-norm of the solution is a constant almost surely (a.s.) (for more details see Theorem 2.2), i.e.,

$$\int_{\Theta} (|\mathbf{E}(x,y,z,t)|^2 + |\mathbf{H}(x,y,z,t)|^2) dxdydz = Constant, \ a.s. \tag{1.3}$$

There have been a lot of ongoing research activities in energy-conserving numerical methods for deterministic Maxwell equations, and various methods have been proposed in the literatures [4,5,14,19]. However, in the stochastic setting, we are only aware of the numerical schemes proposed in [6,9,10,16] for stochastic Hamiltonian ODEs. The authors in [3,11] proposed stochastic multi-symplectic methods for stochastic Maxwell equations with additive noise, which have the merits of preserving the discrete stochastic multi-symplectic conservation law and stochastic energy dissipative properties.

To the best of our knowledge, there has been no reference considering this aspect for stochastic Maxwell equations with multiplicative noise till now. In addition, numerical methods preserving the structure characteristics of equations should be much better in preservation of physical properties and have better stability in numerical computation. Generally speaking, this kind of numerical methods constructed by finite difference techniques is completely implicit for non-separable stochastic system, and demands substantial computational cost. In this paper, we use the idea of wavelet collocation method to get an efficient, multi-symplectic and energy-conserving numerical method. By using this method, we obtain a system of algebraic equations with a sparse differentiation matrix, leading to a numerical algorithm of reduced computational cost. Several numerical examples are presented to show the good behaviors of the proposed method by making comparison with a standard finite difference method. Particularly, numerical experiments demonstrate the mean square convergence order of the proposed numerical method in temporal direction.

The rest of this paper is organized as follows. In section 2, we present some geometric and physical properties of 3D stochastic Maxwell equations with multiplicative noise. It is shown that the phase flow of equations preserves the stochastic multi-symplectic structure of phase space, and the equations possess energy conservation law. In section 3, we propose a numerical method and show that the method preserves discrete energy conservation law and the discrete stochastic multi-symplectic conservation law. In section 4, numerical experiments are performed to testify the effectiveness of the method. Concluding remarks are presented in section 5.

2. Stochastic Maxwell equations

In this section, we will present some preliminary results of 3D stochastic Maxwell equations (1.1). For simplicity in notations, we just consider the case that Wiener process $W(t,x,y,z,\omega)$ is applied in one dimensional spatial direction. Throughout this paper, u_s $(s = t,x,y,z)$ denotes the partial derivative of function u with respect to s, i.e., $u_s = \frac{\partial u}{\partial s}$. $d_t u$ denotes the partial differential of u with respect to t, i.e., $d_t u = \frac{\partial u}{\partial t}dt$.

2.1. Stochastic multi-symplectic structure

A stochastic partial differential equation is called a stochastic Hamiltonian partial differential equation if it can be written in the form [12]

$$Md_t u + K u_x dt = \nabla S_1(u)dt + \nabla S_2(u) \circ dW(t), \ \ u \in \mathbb{R}^d, \tag{2.1}$$

where M and K are skew-symmetric matrices, and S_1 and S_2 are real smooth functions of variable u. Stochastic Maxwell equations with multiplicative noise (1.1) can be written as follows

$$Md_t u + K_1 u_x dt + K_2 u_y dt + K_3 u_z dt = \nabla_u S(u) \circ dW, \ \ u \in \mathbb{R}^6. \tag{2.2}$$

Here,

$$u = \big(H_1, H_2, H_3, E_1, E_2, E_3\big)^T,$$

$$S(u) = \frac{\lambda}{2}\Big(|E_1|^2 + |E_2|^2 + |E_3|^2 + |H_1|^2 + |H_2|^2 + |H_3|^2\Big)$$

and

$$M = \begin{pmatrix} 0 & -I_{3\times 3} \\ I_{3\times 3} & 0 \end{pmatrix}, \quad K_i = \begin{pmatrix} \mathscr{D}_i & 0 \\ 0 & \mathscr{D}_i \end{pmatrix}, \ i = 1,2,3.$$

The sub-matrix $I_{3\times 3}$ is a 3×3 identity matrix and

$$\mathscr{D}_1 = \begin{pmatrix} 0 & 0 & 0 \\ 0 & 0 & -1 \\ 0 & 1 & 0 \end{pmatrix}, \mathscr{D}_2 = \begin{pmatrix} 0 & 0 & 1 \\ 0 & 0 & 0 \\ -1 & 0 & 0 \end{pmatrix}, \mathscr{D}_3 = \begin{pmatrix} 0 & -1 & 0 \\ 1 & 0 & 0 \\ 0 & 0 & 0 \end{pmatrix}.$$

Similarly to the proof of Theorem 2.2 in [12], we have the following result.

Theorem 2.1. *System (2.2) possesses the stochastic multi-symplectic conservation law locally*

$$d_t\omega + \partial_x\kappa_1 dt + \partial_y\kappa_2 dt + \partial_z\kappa_3 dt = 0, \ a.s.,$$

i.e.,

$$\begin{aligned}
&\int_{z_0}^{z_1}\int_{y_0}^{y_1}\int_{x_0}^{x_1} \omega(t_1, x, y, z)dxdydz + \int_{z_0}^{z_1}\int_{y_0}^{y_1}\int_{t_0}^{t_1} \kappa_1(t, x_1, y, z)dtdydz \\
&+ \int_{z_0}^{z_1}\int_{x_0}^{x_1}\int_{t_0}^{t_1} \kappa_2(t, x, y_1, z)dtdxdz + \int_{y_0}^{y_1}\int_{x_0}^{x_1}\int_{t_0}^{t_1} \kappa_3(t, x, y, z_1)dtdxdy \\
&= \int_{z_0}^{z_1}\int_{y_0}^{y_1}\int_{x_0}^{x_1} \omega(t_0, x, y, z)dxdydz + \int_{z_0}^{z_1}\int_{y_0}^{y_1}\int_{t_0}^{t_1} \kappa_1(t, x_0, y, z)dtdydz \\
&+ \int_{z_0}^{z_1}\int_{x_0}^{x_1}\int_{t_0}^{t_1} \kappa_2(t, x, y_0, z)dtdxdz + \int_{y_0}^{y_1}\int_{x_0}^{x_1}\int_{t_0}^{t_1} \kappa_3(t, x, y, z_0)dtdxdy,
\end{aligned}$$

where $\omega(t, x, y, z) = \frac{1}{2}du \wedge Mdu$, $\kappa_i(t, x, y, z) = \frac{1}{2}du \wedge K_i du$ are the differential 2-forms associated with the skew-symmetric matrices M and K_i $(i = 1, 2, 3)$, respectively, and $(t_0, t_1) \times (x_0, x_1) \times (y_0, y_1) \times (z_0, z_1)$ is the local definition domain of $u(t, x, y, z)$.

Remark 1. To avoid confusion, we note that the differentials in equation (2.1) and differential 2-forms ω, κ have different meanings. In (2.1), u are treated as functions of time and the initial value $u(0, x, y, z)$ is fixed parameters, while differentiations in ω and κ are made with respect to the initial data $u(0, x, y, z)$.

2.2. Energy conservation law

As is well known, the deterministic Maxwell equations have the following invariant [4]

$$\int_{\Theta} (|\mathbf{E}(x, y, z, t)|^2 + |\mathbf{H}(x, y, z, t)|^2)dxdydz = Constant. \tag{2.3}$$

This invariant is also called Poynting theorem in electromagnetism and can be easily verified. Similarly, based on the infinite dimensional Itô formula [17], we can also obtain the energy conservation law for system (1.1). This result shows that the electromagnetic energy is still invariant under the multiplicative noise. This is stated in the following Theorem.

Theorem 2.2. *Let $(\mathbf{E}, \mathbf{H})^T$ be the solution of (1.1) under PEC boundary condition (1.2). Then for any $t \in [0, T]$,*

$$\begin{aligned}
\Upsilon(t) &= \int_{\Theta} (|\mathbf{E}(x, y, z, t)|^2 + |\mathbf{H}(x, y, z, t)|^2)dxdydz \\
&= \int_{\Theta} (|\mathbf{E}(x, y, z, t_0)|^2 + |\mathbf{H}(x, y, z, t_0)|^2)dxdydz \\
&= \Upsilon(t_0), \ \ a.s.
\end{aligned} \tag{2.4}$$

Proof. In order to prove the result (2.4), we will use an equivalent Itô form of (1.1). Define a function

$$\Psi(x) = \sum_{m=0}^{\infty} (\sqrt{\eta_m} e_m(x))^2, \ x \in \mathbb{R}, \tag{2.5}$$

which is independent of the basis $\{e_m\}_{m\in\mathbb{N}}$. Then this equivalent Itô equation can be rewritten as

$$\begin{aligned} d\mathbf{E} &= (\nabla\times\mathbf{H} - \frac{1}{2}\lambda^2\Psi\mathbf{E})dt - \lambda\mathbf{H}dW, \\ d\mathbf{H} &= (-\nabla\times\mathbf{E} - \frac{1}{2}\lambda^2\Psi\mathbf{H})dt + \lambda\mathbf{E}dW. \end{aligned} \tag{2.6}$$

Introducing the following functionals

$$F_1(\mathbf{E}) = \int_\Theta |\mathbf{E}(x,y,z,t)|^2 dxdydz,$$

$$F_2(\mathbf{H}) = \int_\Theta |\mathbf{H}(x,y,z,t)|^2 dxdydz.$$

It is easy to verify that **E** and **H** satisfy the following first and second Fréchet derivative

$$\begin{aligned} DF_1(\mathbf{E})(\varphi) &= 2\int_\Theta \langle \mathbf{E},\varphi\rangle dxdydz, \quad D^2F_1(\mathbf{E})(\varphi,\psi) = 2\int_\Theta \langle\psi,\varphi\rangle dxdydz, \\ DF_2(\mathbf{H})(\varphi) &= 2\int_\Theta \langle \mathbf{H},\varphi\rangle dxdydz, \quad D^2F_2(\mathbf{H})(\varphi,\psi) = 2\int_\Theta \langle\psi,\varphi\rangle dxdydz, \end{aligned} \tag{2.7}$$

where $\varphi,\psi\in L^2(\Theta)^3$, and $\langle\cdot,\cdot\rangle$ denotes the Euclidean inner product.

Based on the system (2.6), the infinite dimensional Itô formula for $F_1(\mathbf{E}(t))$ leads to

$$\begin{aligned} F_1(\mathbf{E}(t)) =& F_1(\mathbf{E}(0)) + 2\int_\Theta\int_0^t \langle \mathbf{E}(s), -\lambda\mathbf{H}(s)dW(s)\rangle dxdydz \\ &+ 2\int_\Theta\int_0^t \langle \mathbf{E}(s), \nabla\times\mathbf{H}(s) - \frac{1}{2}\lambda^2\Psi\mathbf{E}(s)\rangle dsdxdydz \\ &+ \lambda^2\int_\Theta\int_0^t Tr[\langle \mathbf{H}(s),\mathbf{H}(s)\rangle Q^{\frac{1}{2}}(Q^{\frac{1}{2}})^*]dsdxdydz. \end{aligned} \tag{2.8}$$

Similarly, we apply Itô formula to $F_2(\mathbf{H}(t))$ and obtain

$$\begin{aligned} F_2(\mathbf{H}(t)) =& F_2(\mathbf{H}(0)) + 2\int_\Theta\int_0^t \langle \mathbf{H}(s), \lambda\mathbf{E}(s)dW(s)\rangle dxdydz \\ &- 2\int_\Theta\int_0^t \langle \mathbf{H}(s), \nabla\times\mathbf{E}(s) + \frac{1}{2}\lambda^2\Psi\mathbf{H}(s)\rangle dsdxdydz \\ &+ \lambda^2\int_\Theta\int_0^t Tr[\langle \mathbf{E}(s),\mathbf{E}(s)\rangle Q^{\frac{1}{2}}(Q^{\frac{1}{2}})^*]dsdxdydz. \end{aligned} \tag{2.9}$$

Summing (2.8) and (2.9), then we have

$$\begin{aligned} \int_\Theta (|\mathbf{E}(t)|^2 + |\mathbf{H}(t)|^2)dxdydz =& \int_\Theta (|\mathbf{E}(0)|^2 + |\mathbf{H}(0)|^2)dxdydz \\ &+ 2\underbrace{\int_\Theta\int_0^t \langle \mathbf{E}(s),\nabla\times\mathbf{H}(s)\rangle - \langle \mathbf{H}(s),\nabla\times\mathbf{E}(s)\rangle dsdxdydz}_{C} \end{aligned}$$

$$+\underbrace{\int_{\Theta}\int_0^t \langle \mathbf{E}(s), -\lambda^2\Psi\mathbf{E}(s)\rangle + \langle \mathbf{H}(s), -\lambda^2\Psi\mathbf{H}(s)\rangle dsdxdydz}_{D}$$

$$+\underbrace{\int_{\Theta}\int_0^t \lambda^2\langle \mathbf{H}(s), \mathbf{H}(s)\rangle Tr(Q) + \lambda^2\langle \mathbf{E}(s), \mathbf{E}(s)\rangle Tr(Q) dsdxdydz}_{P}.$$

Here $Tr(Q)$ denotes the trace of operate Q. By Green's formula and PEC boundary condition (1.2), the term C satisfies the following equality

$$\begin{aligned}
C &= -\int_0^t\int_{\Theta} \nabla\cdot(\mathbf{E}\times\mathbf{H})dxdydzds \\
&= -\int_0^t\int_{\partial\Theta} (\mathbf{E}\times\mathbf{H})\cdot\mathbf{n}dxdydzds \\
&= 0.
\end{aligned}$$

It follows from the definition of Ψ that $D + P = 0$. Thus, we can get the energy conservation law (2.4). □

Remark 2. Equality (2.4) is an important criterion in constructing efficient numerical methods for computing the propagation of electromagnetic wave and in measuring whether a numerical simulation method is good or not.

Remark 3. From the expression (2.4), it seems same as the deterministic case. However, the energy of stochastic Maxwell equation is conserved in sense of almost surely, that is to say, it holds for any ω outside a set of measure 0.

3. Energy-conserving method

In this section, we propose an energy-conserving numerical method for (1.1). It is a combination of midpoint method in time and wavelet collocation method in space.

3.1. Discretization in time and space

Applying the midpoint method to equation (1.1) in temporal direction, we get

$$\begin{aligned}
H_1^{n+1} &= H_1^n + \Delta t\Big(\frac{\partial}{\partial z}E_2^{n+1/2} - \frac{\partial}{\partial y}E_3^{n+1/2}\Big) + \lambda E_1^{n+1/2}\Delta W^n, \\
H_2^{n+1} &= H_2^n + \Delta t\Big(\frac{\partial}{\partial x}E_3^{n+1/2} - \frac{\partial}{\partial z}E_1^{n+1/2}\Big) + \lambda E_2^{n+1/2}\Delta W^n, \\
H_3^{n+1} &= H_3^n + \Delta t\Big(\frac{\partial}{\partial y}E_1^{n+1/2} - \frac{\partial}{\partial x}E_2^{n+1/2}\Big) + \lambda E_3^{n+1/2}\Delta W^n, \\
E_1^{n+1} &= E_1^n - \Delta t\Big(\frac{\partial}{\partial z}H_2^{n+1/2} - \frac{\partial}{\partial y}H_3^{n+1/2}\Big) - \lambda H_1^{n+1/2}\Delta W^n, \\
E_2^{n+1} &= E_2^n - \Delta t\Big(\frac{\partial}{\partial x}H_3^{n+1/2} - \frac{\partial}{\partial z}H_1^{n+1/2}\Big) - \lambda H_2^{n+1/2}\Delta W^n, \\
E_3^{n+1} &= E_3^n - \Delta t\Big(\frac{\partial}{\partial y}H_1^{n+1/2} - \frac{\partial}{\partial x}H_2^{n+1/2}\Big) - \lambda H_3^{n+1/2}\Delta W^n,
\end{aligned} \tag{3.1}$$

where Δt is the temporal step-size and $u^{n+1/2} = \frac{1}{2}(u^n + u^{n+1})$. In the sequel,

$$\Delta W^n = W(t_{n+1}) - W(t_n) = \sum_{m=1}^{\mathscr{M}} \sqrt{\eta_m}(\beta_m(t_{n+1}) - \beta_m(t_n))e_m, \tag{3.2}$$

where $\mathscr{M}$ is a positive integer.

Now, we apply wavelet collocation method to discretize (3.1) in spatial direction and obtain the full-discrete stochastic multi-symplectic wavelet collocation method. Firstly, we give some preliminary results of wavelet collocation method.

In [7], Daubechies introduced compactly supported wavelets which proved to be very useful in numerical analysis. In this paper, the autocorrelation functions of Daubechies scaling functions will be used as trial functions, which make the first-order differentiation matrix be skew-symmetric and sparse. A Daubechies scaling function $\phi(x)$ of order γ satisfies (see [1])

$$\phi(x) = \sum_{k=0}^{\gamma-1} h_k \phi(2x-k), \tag{3.3}$$

where γ is a positive even integer and $\{h_k\}_{k=0}^{\gamma-1}$ are γ non-vanishing "filter coefficients". Define the autocorrelation function $\theta(x)$ of $\phi(x)$ as

$$\theta(x) = \int \phi(x)\phi(t-x)dt. \tag{3.4}$$

Such autocorrelation function θ verifies trivially the equality $\theta(n) = \delta_{0n}$. Suppose that V_j is the linear span of $\{\theta_{jk}(x) = 2^{j/2}\theta(2^j x - k), k \in \mathbb{Z}\}$. It can be proved that $(V_j)_{j\in\mathbb{Z}}$ forms a multiresolution analysis.

Consider $E_1(x, y, z, t)$ defined on spatial domain $[0, L_1] \times [0, L_2] \times [0, L_3]$ with $N_1 \times N_2 \times N_3$ grid points, where $N_1 = L_1 \cdot 2^{J_1}$, $N_2 = L_2 \cdot 2^{J_2}$, $N_3 = L_3 \cdot 2^{J_3}$. Interpolating it at collocation points $(x_i, y_j, z_k) = (i/2^{J_1}, j/2^{J_2}, k/2^{J_3})$, $i = 1, ..., N_1$, $j = 1, ..., N_2$, $k = 1, ..., N_3$ gives

$$IE_1(x, y, z, t) = \sum_{i=1}^{N_1}\sum_{j=1}^{N_2}\sum_{k=1}^{N_3} E_{1_{i,j,k}} \theta(2^{J_1}x - i)\theta(2^{J_2}y - j)\theta(2^{J_3}z - k), \tag{3.5}$$

where IE_1 stands for the interpolation of E_1 using the basis functions. Making partial differential with respect to y and evaluating the resulting expression at collocation points, we obtain

$$\begin{aligned}
\frac{\partial IE_1(x_i, y_j, z_k, t)}{\partial y} &= \sum_{i'=1}^{N_1}\sum_{j'=1}^{N_2}\sum_{k'=1}^{N_3} E_{1_{i',j',k'}} \theta(2^{J_1}x_i - i')\theta(2^{J_3}z_k - k')\frac{d\theta(2^{J_2}y - j')}{dy}|_{y_j} \\
&= \sum_{j'=1}^{N_2} E_{1_{i,j',k}} (2^{J_2}\theta'(j - j')) = \sum_{j'=j-(\gamma-1)}^{j+(\gamma-1)} E_{1_{i,j',k}} (B^y)_{j,j'} \\
&= ((I_{N_1} \otimes B^y \otimes I_{N_3})\mathbf{E}_1)_{i,j,k},
\end{aligned}$$

where $\otimes$ means Kronecker inner product and I_{N_1} is the $N_1 \times N_1$ identity matrix. $\mathbf{E_1} = ((E_1)_{1,1,1}, (E_1)_{2,1,1}, (E_1)_{N_1,1,1}, \cdots, (E_1)_{1,N_2,1}, \cdots, (E_1)_{N_1,N_2,N_3})^T$. The differential matrix B^y for the first-order partial differential operator ∂_y is an $N_2 \times N_2$ sparse skew-symmetric circulant matrix with entries

$$(B^y)_{m,m'} = \begin{cases} 2^{J_2}\theta'(m - m'), & m - (\gamma - 1) \le m' \le m + (\gamma - 1); \\ 2^{J_2}\theta'(-l), & m - m' = N_2 - l, \quad 1 \le l \le \gamma - 1; \\ 2^{J_2}\theta'(l), & m' - m = N_2 - l, \quad 1 \le l \le \gamma - 1; \\ 0, & \text{otherwise}. \end{cases}$$

Using the similar manner, we can obtain the discrete differential matrices $B^x \otimes I_{N_2} \otimes I_{N_3}$ and $I_{N_1} \otimes I_{N_2} \otimes B^z$ corresponding to ∂_x and ∂_z, respectively. Now we have a full-discrete method for stochastic Maxwell equations as

$$\begin{aligned}
(\mathbf{E_1})^{n+1} - (\mathbf{E_1})^n &= \Delta t\Big(A_2(\mathbf{H_3})^{n+1/2} - A_3(\mathbf{H_2})^{n+1/2}\Big) - \lambda(\mathbf{H_1})^{n+1/2}\mathbf{W}^n, \\
(\mathbf{E_2})^{n+1} - (\mathbf{E_2})^n &= \Delta t\Big(A_3(\mathbf{H_1})^{n+1/2} - A_1(\mathbf{H_3})^{n+1/2}\Big) - \lambda(\mathbf{H_2})^{n+1/2}\mathbf{W}^n, \\
(\mathbf{E_3})^{n+1} - (\mathbf{E_3})^n &= \Delta t\Big(A_1(\mathbf{H_2})^{n+1/2} - A_2(\mathbf{H_1})^{n+1/2}\Big) - \lambda(\mathbf{H_3})^{n+1/2}\mathbf{W}^n, \\
(\mathbf{H_1})^{n+1} - (\mathbf{H_1})^n &= \Delta t\Big(A_3(\mathbf{E_2})^{n+1/2} - A_2(\mathbf{E_3})^{n+1/2}\Big) + \lambda(\mathbf{E_1})^{n+1/2}\mathbf{W}^n, \\
(\mathbf{H_2})^{n+1} - (\mathbf{H_2})^n &= \Delta t\Big(A_1(\mathbf{E_3})^{n+1/2} - A_3(\mathbf{E_1})^{n+1/2}\Big) + \lambda(\mathbf{E_2})^{n+1/2}\mathbf{W}^n, \\
(\mathbf{H_3})^{n+1} - (\mathbf{H_3})^n &= \Delta t\Big(A_2(\mathbf{E_1})^{n+1/2} - A_1(\mathbf{E_2})^{n+1/2}\Big) + \lambda(\mathbf{E_3})^{n+1/2}\mathbf{W}^n,
\end{aligned} \tag{3.6}$$

where $A_1 = B^x \otimes I_{N_2} \otimes I_{N_3}$, $A_2 = I_{N_1} \otimes B^y \otimes I_{N_3}$ and $A_3 = I_{N_1} \otimes I_{N_2} \otimes B^z$ are skew-symmetric, $\mathbf{W}^n = \mathbf{e} \otimes (\Delta W_1^n, \cdots, \Delta W_{N_1}^n)^T$, $\mathbf{e} = (1, 1, \cdots, 1, 1)^T_{N_2 \times N_3}$, ΔW_i^n is an approximation of ΔW^n in spatial direction with respect to x. And $(\mathbf{H_1})^{n+1/2}\mathbf{W}^n$ denotes the components multiplication between $(\mathbf{H_1})^{n+1/2}$ and $\mathbf{W}^n$, respectively.

3.2. Properties of the method

In this section, we show that the method (3.6) preserves the discrete stochastic multi-symplectic conservation law and discrete energy conservation law.

3.2.1. Stochastic multi-symplecticity

The discrete stochastic multi-symplectic conservation law is stated as follows.

Theorem 3.1. *The method (3.6) has the following discrete stochastic multi-symplectic conservation law*

$$\begin{aligned}\frac{\omega_{i,j,k}^{n+1} - \omega_{i,j,k}^n}{\Delta t} &+ \sum_{i'=i-(\gamma-1)}^{i+(\gamma-1)} (B^x)_{i,i'} (\kappa_x)_{i',j,k}^{n+1/2} \\ &+ \sum_{j'=j-(\gamma-1)}^{j+(\gamma-1)} (B^y)_{j,j'} (\kappa_y)_{i,j',k}^{n+1/2} + \sum_{k'=k-(\gamma-1)}^{k+(\gamma-1)} (B^z)_{k,k'} (\kappa_z)_{i,j,k'}^{n+1/2} = 0,\end{aligned} \tag{3.7}$$

where

$$\omega_{i,j,k}^n = \frac{1}{2} d\mathbf{u}_{i,j,k}^n \wedge M d\mathbf{u}_{i,j,k}^n, \quad (\kappa_x)_{i',j,k}^{n+1/2} = d\mathbf{u}_{i,j,k}^{n+1/2} \wedge K_1 d\mathbf{u}_{i',j,k}^{n+1/2},$$

$$(\kappa_y)_{i,j',k}^{n+1/2} = d\mathbf{u}_{i,j,k}^{n+1/2} \wedge K_2 d\mathbf{u}_{i,j',k}^{n+1/2}, \quad (\kappa_z)_{i,j,k'}^{n+1/2} = d\mathbf{u}_{i,j,k}^{n+1/2} \wedge K_3 d\mathbf{u}_{i,j,k'}^{n+1/2}.$$

Proof. Let $\mathbf{u} = (\mathbf{H_1}, \mathbf{H_2}, \mathbf{H_3}, \mathbf{E_1}, \mathbf{E_2}, \mathbf{E_3})^T$. (3.6) can be rewritten as

$$\begin{aligned}M\frac{\mathbf{u}_{i,j,k}^{n+1} - \mathbf{u}_{i,j,k}^n}{\Delta t} &+ \sum_{i'=i-(\gamma-1)}^{i+(\gamma-1)} (B^x)_{i,i'} (K_1 \mathbf{u}_{i',j,k}^{n+1/2}) + \sum_{j'=j-(\gamma-1)}^{j+(\gamma-1)} (B^y)_{j,j'} (K_2 \mathbf{u}_{i,j',k}^{n+1/2}) \\ &+ \sum_{k'=k-(\gamma-1)}^{k+(\gamma-1)} (B^z)_{k,k'} (K_3 \mathbf{u}_{i,j,k'}^{n+1/2}) = \nabla_{\mathbf{u}} S(\mathbf{u}_{i,j,k}^{n+1/2}) \frac{\Delta W_i^n}{\Delta t}.\end{aligned}$$

The variational form associated with the above equation is

$$\begin{aligned}M\frac{d\mathbf{u}_{i,j,k}^{n+1} - d\mathbf{u}_{i,j,k}^n}{\Delta t} &+ \sum_{i'=i-(\gamma-1)}^{i+(\gamma-1)} (B^x)_{i,i'} (K_1 d\mathbf{u}_{i',j,k}^{n+1/2}) + \sum_{j'=j-(\gamma-1)}^{j+(\gamma-1)} (B^y)_{j,j'} (K_2 d\mathbf{u}_{i,j',k}^{n+1/2}) \\ &+ \sum_{k'=k-(\gamma-1)}^{k+(\gamma-1)} (B^z)_{k,k'} (K_3 d\mathbf{u}_{i,j,k'}^{n+1/2}) = \nabla^2 S(\mathbf{u}_{i,j,k}^{n+1/2}) d\mathbf{u}_{i,j,k}^{n+1/2} \frac{\Delta W_i^n}{\Delta t}.\end{aligned}$$

Taking the wedge product with $d\mathbf{u}_{i,j,k}^{n+1/2}$ on both sides of the above equation, we can get the stochastic multi-symplectic conservation law (3.7). □

3.2.2. Energy preservation

In this subsection, we will state the discrete energy conservation law.

Theorem 3.2. *Under periodic boundary conditions, the stochastic multi-symplectic wavelet collocation method (3.6) has the following discrete energy conservation law*

$$\|\mathbf{E}^n\|^2 + \|\mathbf{H}^n\|^2 = Constant, \ a.s., \tag{3.8}$$

where

$$\|\mathbf{E}^n\|^2 = \Delta x \Delta y \Delta z \sum_{i=1}^{N_1} \sum_{j=1}^{N_2} \sum_{k=1}^{N_3} \Big((E_{1_{i,j,k}}^n)^2 + (E_{2_{i,j,k}}^n)^2 + (E_{3_{i,j,k}}^n)^2 \Big),$$

$$\|\mathbf{H}^n\|^2 = \Delta x \Delta y \Delta z \sum_{i=1}^{N_1}\sum_{j=1}^{N_2}\sum_{k=1}^{N_3}\Big((H^n_{1_{i,j,k}})^2 + (H^n_{2_{i,j,k}})^2 + (H^n_{3_{i,j,k}})^2\Big).$$

Proof. We make inner product of (3.6) with $\mathbf{E}_1^{n+1/2}$, $\mathbf{E}_2^{n+1/2}$, $\mathbf{E}_3^{n+1/2}$, $\mathbf{H}_1^{n+1/2}$, $\mathbf{H}_2^{n+1/2}$, $\mathbf{H}_3^{n+1/2}$, respectively, it yields

$$\frac{\|\mathbf{E}_1^{n+1}\|^2 - \|\mathbf{E}_1^n\|^2}{2} = \langle (A_2\mathbf{H}_3^{n+1/2} - A_3\mathbf{H}_2^{n+1/2}), \mathbf{E}_1^{n+1/2}\rangle \Delta t - \lambda\langle \mathbf{H}_1^{n+1/2}\mathbf{W}^n, \mathbf{E}_1^{n+1/2}\rangle,$$

$$\frac{\|\mathbf{E}_2^{n+1}\|^2 - \|\mathbf{E}_2^n\|^2}{2} = \langle (A_3\mathbf{H}_1^{n+1/2} - A_1\mathbf{H}_3^{n+1/2}), \mathbf{E}_2^{n+1/2}\rangle \Delta t - \lambda\langle \mathbf{H}_2^{n+1/2}\mathbf{W}^n, \mathbf{E}_2^{n+1/2}\rangle,$$

$$\frac{\|\mathbf{E}_3^{n+1}\|^2 - \|\mathbf{E}_3^n\|^2}{2} = \langle (A_1\mathbf{H}_2^{n+1/2} - A_2\mathbf{H}_1^{n+1/2}), \mathbf{E}_3^{n+1/2}\rangle \Delta t - \lambda\langle \mathbf{H}_3^{n+1/2}\mathbf{W}^n, \mathbf{E}_3^{n+1/2}\rangle,$$

$$\frac{\|\mathbf{H}_1^{n+1}\|^2 - \|\mathbf{H}_1^n\|^2}{2} = \langle (A_3\mathbf{E}_2^{n+1/2} - A_2\mathbf{E}_3^{n+1/2}), \mathbf{H}_1^{n+1/2}\rangle \Delta t + \lambda\langle \mathbf{E}_1^{n+1/2}\mathbf{W}^n, \mathbf{H}_1^{n+1/2}\rangle,$$

$$\frac{\|\mathbf{H}_2^{n+1}\|^2 - \|\mathbf{H}_2^n\|^2}{2} = \langle (A_1\mathbf{E}_3^{n+1/2} - A_3\mathbf{E}_1^{n+1/2}), \mathbf{H}_2^{n+1/2}\rangle \Delta t + \lambda\langle \mathbf{E}_2^{n+1/2}\mathbf{W}^n, \mathbf{H}_2^{n+1/2}\rangle,$$

$$\frac{\|\mathbf{H}_3^{n+1}\|^2 - \|\mathbf{H}_3^n\|^2}{2} = \langle (A_2\mathbf{E}_1^{n+1/2} - A_1\mathbf{E}_2^{n+1/2}), \mathbf{H}_3^{n+1/2}\rangle \Delta t + \lambda\langle \mathbf{E}_3^{n+1/2}\mathbf{W}^n, \mathbf{H}_3^{n+1/2}\rangle.$$

In addition, noticing that A_1, A_2, A_3 are skew-symmetric matrices, we sum all terms in the above equations and obtain

$$\frac{1}{2}\Big[(\|\mathbf{E}^{n+1}\|^2 + \|\mathbf{H}^{n+1}\|^2) - (\|\mathbf{E}^n\|^2 + \|\mathbf{H}^n\|^2)\Big] = 0,$$

which leads to the energy conservation law (3.8). □

The result of this theorem is evidently consistent with (2.4), which means that the energy can be preserved by the proposed stochastic multi-symplectic wavelet collocation method. In the next section, we will verify this conservation law numerically.

4. Numerical results

In this section we provide four numerical experiments to illustrate the accuracy and capability of the method developed in the previous sections. We investigate the good performance of the stochastic multi-symplectic wavelet collocation method, compared with a central finite difference method. Furthermore, we check the temporal accuracy by fixing the space step sufficiently small such that errors stemming from the spatial approximation are negligible.

When we take no account of the noise term, i.e., $\lambda = 0$, (1.1) reduces to 3D deterministic Maxwell equations. In our numerical calculations, initial values

$$\begin{aligned} &E_{1_0} = \cos(2\pi(x+y+z)),\ E_{2_0} = -2E_{1_0},\ E_{3_0} = E_{1_0},\\ &H_{1_0} = \sqrt{3}E_{1_0},\ H_{2_0} = 0,\ H_{3_0} = -\sqrt{3}E_{1_0} \end{aligned} \tag{4.1}$$

on $\Theta = [0,1]^3$ and periodic boundary conditions are considered. In the following numerical experiments, we use the order of the Daubechies scaling function $\gamma = 4$ and the uniform spatial stepsize $\Delta x = \Delta y = \Delta z = h$ to solve the problem. And we take the orthonormal basis $\{e_m\}_{m\in\mathbb{N}}$ and eigenvalue $(\eta_m)_{m\in\mathbb{N}}$ as

$$e_m(x) = \sqrt{2}\sin(m\pi x),\quad \eta_m = \frac{1}{m^2}, \tag{4.2}$$

then ΔW_i^n can be regarded as an approximation of integral

$$\Delta W_i^n = \frac{1}{\Delta x}\int_{i\Delta x}^{(i+1)\Delta x}\int_{t_n}^{t_{n+1}}\sum_{m=1}^{\infty}\sqrt{\eta_m}e_m(x)d\beta_m(s)dx. \tag{4.3}$$

Substituting (4.2) into (4.3) yields

$$\Delta W_i^n = \frac{1}{\Delta x}\sum_{m=1}^{\infty}\frac{\sqrt{2\eta_m}}{m\pi}\Big[\cos(m\pi i\Delta x) - \cos(m\pi(i+1)\Delta x)\Big]\Big[\beta_m(t_{n+1}) - \beta_m(t_n)\Big],$$

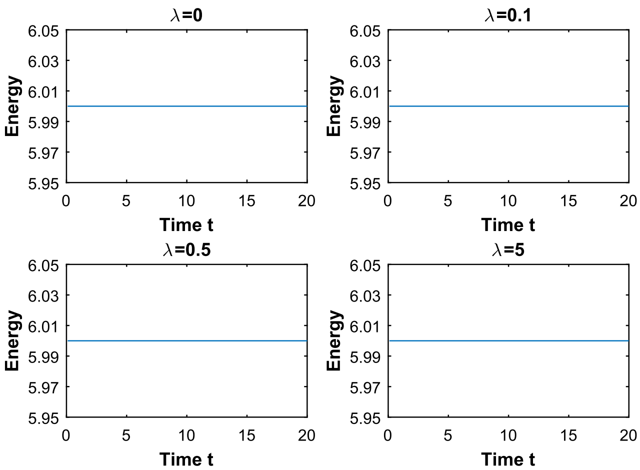

Fig. 1. Evolution of the energy over one trajectory until $T = 20$ with $\Delta t = 0.1, h = 1/2^4$ as $\lambda = 0$, $\lambda = 0.5$, $\lambda = 1$ and $\lambda = 5$, respectively.

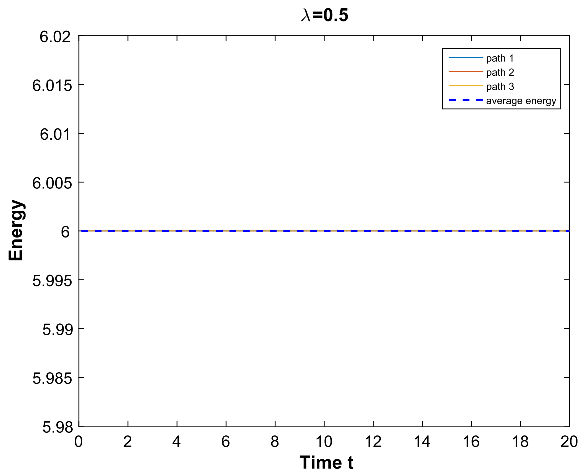

Fig. 2. Evolution of average discrete energy along 100 trajectories and discrete energy over one trajectory as $\lambda = 0.5$, $\Delta t = 0.1, h = 1/2^4$.

where $(\beta_m(t_{n+1}) - \beta_m(t_n))/\sqrt{\Delta t}$ is a sequence of independent and $\mathcal{N}(0, 1)$ distributed random variables. In the sequel, we truncate the infinite series of real-valued Wiener process till $\mathcal{M} = 200$.

Example 1. Energy conservation law.

As is stated in Theorem 3.2, the stochastic multi-symplectic wavelet collocation method (3.6) could preserve the discrete energy conservation law almost surely. We consider this phenomenon numerically in Fig. 1, where it shows the evolution of the discrete energy conservation law in the case of $\lambda = 0,\ 0.5,\ 1.0$ and 5. Although different sizes of noise are chosen, the figures of the discrete energy conservation law remain to be horizontal lines approximately. We observe a good agreement with the theoretical result.

Meanwhile, we also interested in the behavior of average energy. Thus, in Fig. 2, we plot the energy evolution of one trajectory, and the average energy evolution over 100 trajectories till $T = 20$ with $\lambda = 0.5, \Delta t = 0.1, h = 1/2^4$, where the blue lines represent three samples of the profiles, and the red line denotes the evolution of the average discrete energy over 100 trajectories, respectively. From this figure, it can be seen that the averaged energy is nearly horizontal line with respect to time, which coincides with the continuous case.

In order to further investigate the energy conservative property under various cases, we define the following energy error form

$$\text{Energy error} := \Upsilon^n - \Upsilon^0,$$

where Υ^n denotes the discrete energy at time-step t^n. Figs. 3, 4, 5 and 6 show the global energy error with various time steps Δt, spatial resolutions h and sizes of noise λ till $T = 20$, respectively. It can be seen that, the global residuals of the

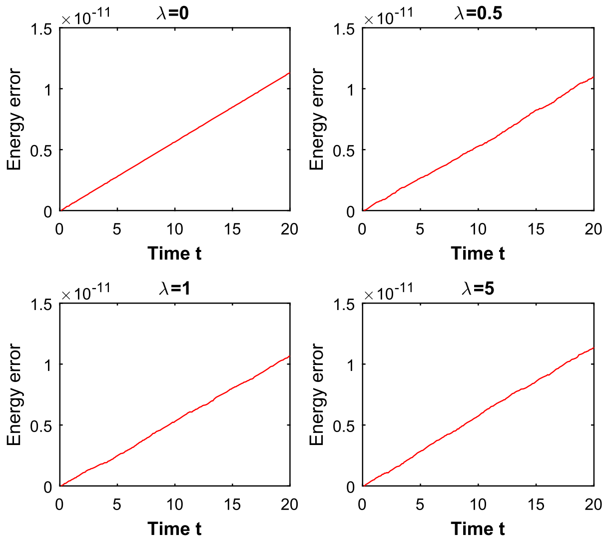

Fig. 3. The global errors of discrete energy over 10 trajectories until $T = 20$ with $\Delta t = 0.1, h = 1/2^4$, respectively.

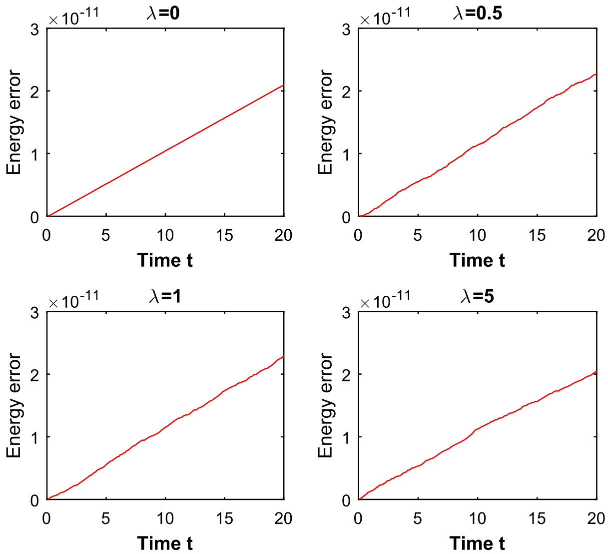

Fig. 4. The global errors of discrete energy over 10 trajectories until $T = 20$ with $\Delta t = 0.1, h = 1/2^5$, respectively.

discrete energy conservation law all reach the magnitude of 10^{-11} for various parameters. Due to the existence of rounding error and the application of iteration method in solver, it leads to the error of energy can not reach the ideal machine accuracy and the energy error increases linearly. Therefore, it is reasonable to say that the proposed method preserves the discrete energy conservation law.

Example 2. Energy boundedness and long-time behavior.

Firstly, we focus on the behavior of maximum modules of discrete energy, i.e., $\max_n(\|\mathbf{E}^n\|^2 + \|\mathbf{H}^n\|^2)$. Fig. 7 displayed the probability density function of maximum energy over 100 trajectories with $\lambda = 0.5, \Delta t = 0.1, h = 1/2^5$. From this figure, we may observe that the averaged energy is bounded. This result can be easily obtained from energy conservation law.

We are also interested in the long-time behavior of the proposed stochastic multi-symplectic wavelet collocation method. In Fig. 8, we plot the global energy error until $T = 1000$ over one trajectory for different sizes of noise $\lambda = 0,\ 0.5,\ 1,\ 5$ with large time step $\Delta t = 0.1$ and low spatial resolution $h = 1/2^4$. From this figure, we observe that the discrete energy error can be controlled in the scale of 10^{-10} and it seems to be getting bigger than the one at $T = 20$. This phenomena is due to the long time accumulation of rounding errors. Therefore, we can say that our method owns long-time computational stability.

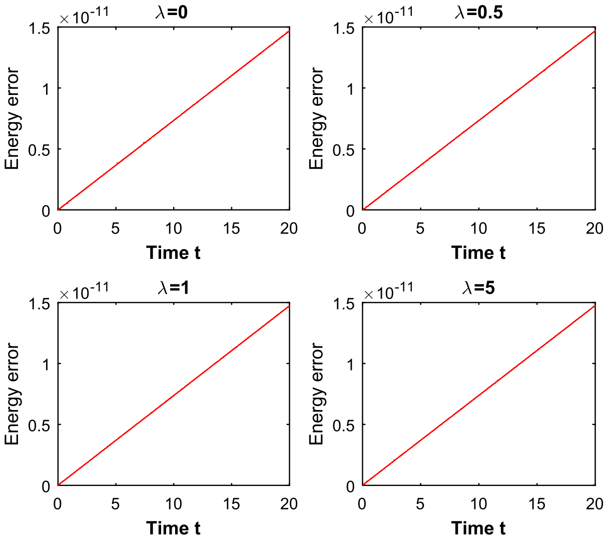

Fig. 5. The global errors of discrete energy over 10 trajectories until $T = 20$ with $\Delta t = 0.005, h = 1/2^4$, respectively.

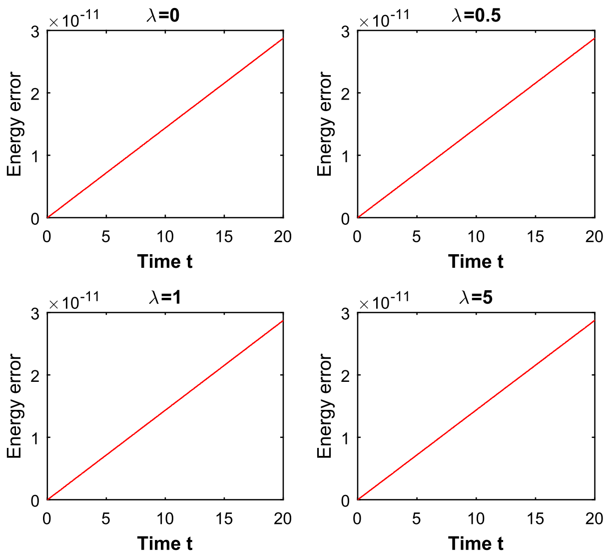

Fig. 6. The global errors of discrete energy over 10 trajectories until $T = 20$ with $\Delta t = 0.005, h = 1/2^5$, respectively.

Example 3. Comparison with finite difference method.

To compare the stochastic multi-symplectic wavelet collocation method in terms of solution behavior, we apply the central finite difference method to discrete stochastic Maxwell equations (1.1). And we define the following normalized energy

$$\text{Normalized energy} := (\Upsilon^n - \Upsilon^0) \times 10^7,$$

where Υ^n and Υ^0 denote the discrete energy at t_n and t_0, respectively. Fig. 9 exhibits the discrete averaged normalized energy over 100 trajectories till $T = 10$ with $\lambda = \sqrt{2}$. We observe that the wavelet collocation method preserves the energy very well. However, the discrete averaged normalized energy obtained by finite difference method shows a rapid growth as time evolves. Furthermore, we plot the energy errors of the two methods in Fig. 10. From the figure, it can be seen that the proposed method is more accurate than the finite difference method in the preservation of energy.

Example 4. Convergence order.

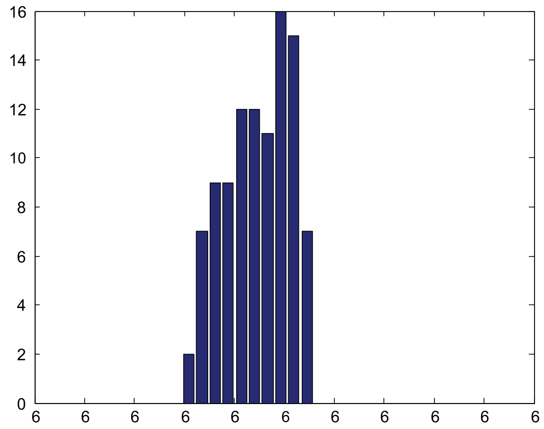

Fig. 7. The probability density function of $\max_n(\|\mathbf{E}^n\|^2 + \|\mathbf{H}^n\|^2)$ in the sense of L^2.

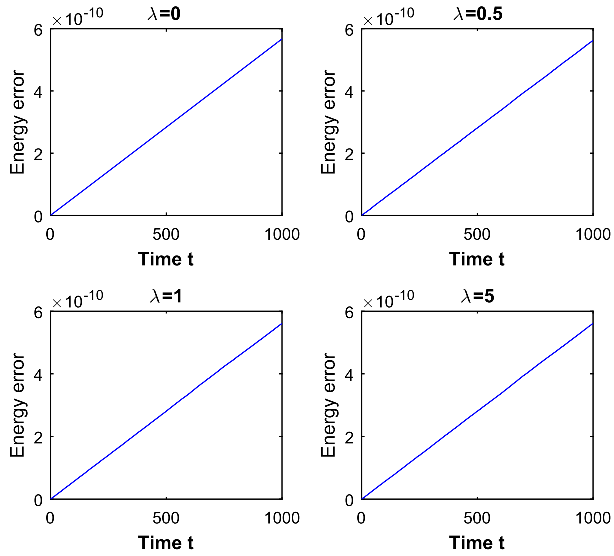

Fig. 8. The global energy errors over one trajectory until $T = 1000$ with $\Delta t = 0.1, h = 1/2^4$.

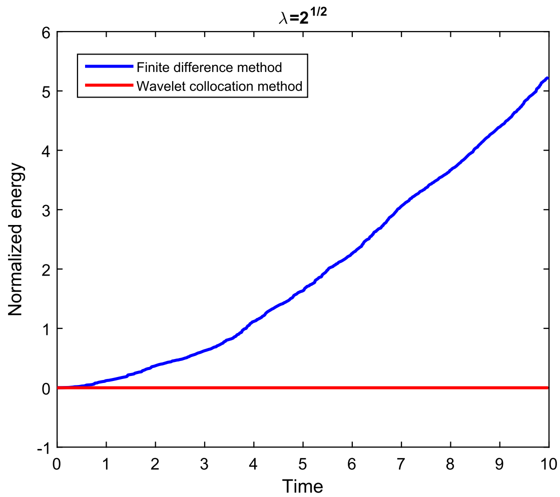

Fig. 9. Evolution of the energy averaged over 100 trajectories with $\Delta t = 1/64, h = 1/2^4$.

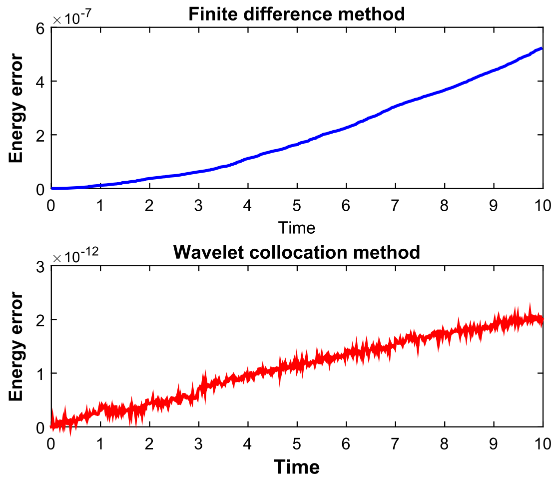

Fig. 10. Evolution of the averaged energy error over 100 trajectories with $\Delta t = 1/64, h = 1/2^4$. Top: finite difference method; Bottom: wavelet collocation method.

Table 1
Accuracy test for stochastic Maxwell equations (1.1).

Δt	L^2 error	Order
$1/2^6$	6.39E-2	–
$1/2^7$	1.60E-2	1.99
$1/2^8$	4.00E-3	2.02
$1/2^9$	9.00E-4	2.07
$1/2^{10}$	2.00E-4	2.32

Table 2
Accuracy test for stochastic Maxwell equations (1.1).

Δt	L^2 error	Order	L^2 error	Order	L^2 error	Order
	$\mathscr{M}=1$		$\mathscr{M}=4$		$\mathscr{M}=8$	
$1/2^6$	3.03E-1	–	4.63E-1	–	6.51E-1	–
$1/2^7$	1.32E-1	1.19	1.95E-1	1.25	2.67E-1	1.29
$1/2^8$	5.78E-2	1.20	8.43E-2	1.21	1.11E-1	1.26
$1/2^9$	2.41E-2	1.26	3.50E-2	1.27	4.48E-2	1.31
$1/2^{10}$	8.20E-3	1.56	1.19E-2	1.56	1.53E-2	1.55

We investigate the convergence order in temporal direction of the proposed stochastic multi-symplectic wavelet collocation method in this experiment. Define

$$e_{\Delta t}^{strong} := \left(\mathbb{E}\|u(\cdot, T) - u_T(\cdot)\|^2\right)^{\frac{1}{2}},$$

with $u = (\mathbf{E}, \ \mathbf{H})^T$. Let $h = 1/2^5, T = 0.1$ and plot $e_{\Delta t}^{strong}$ against Δt on a log-log scale for the truncated number of Wiener process $1 \le \mathscr{M} \le 8$. Although we do not know the explicit form of the solution to (1.1), we take the stochastic multi-symplectic wavelet collocation method with small time stepsize $\Delta t = 2^{-11}$ as the reference solution.

We consider $\lambda = 0$ first: The $e_{\Delta t}^{strong}$ and the convergence orders of the wavelet collocation method in time are listed in Table 1. We can see that the method gives a uniform second order of accuracy for deterministic Maxwell equations.

The observations are different in the stochastic case ($\lambda = \sqrt{2}$) where different sorts of Wiener processes depending on $\mathscr{M}$ are used. Table 2 presents the mean-square convergence order for the L^2-error $e_{\Delta t}^{strong}$. And 100 realizations are chosen to approximate the expectations. As is displayed in Table 2, the strong order of convergence $e_{\Delta t}^{strong}$ is approximately 1 for values 1 to 8 of various sizes of $\mathscr{M}$. It is an interesting and open problem to investigate theoretically the convergence order of the proposed stochastic multi-symplectic wavelet collocation method.

5. Conclusions

In this paper, we design an energy-conserving numerical method for 3D stochastic Maxwell equations with multiplicative noise. The method not only solves equations efficiently, but also preserves exactly the discrete stochastic multi-symplectic conservation law and the discrete energy conservation law. Numerical experiments show the good performance of the proposed method. In addition, the mean square convergence order in time is studied numerically. Since the theoretical analysis of the convergence is difficult, we will devote to study it rigorously in the future work. Certainly, it is also very interesting to extend the method to other equations, such as 3D stochastic nonlinear Schrödinger equation with multiplicative noise.

Acknowledgements

The first and second authors are supported by the NNSFC (NO. 91130003, NO. 11021101, NO. 11290142, NO. 91630312, NO. 11471310, NO. 11601032), the third author is supported by the NNSFC (NO. 11601514 and NO. 11626228), the fourth author is supported by the foundation of Jiangsu Key Laboratory for Numerical Simulation of Large Scale Complex Systems (201606).

References

[1] S. Bertoluzza, G. Naldi, A wavelet collocation method for the numerical solution of partial differential equations, Appl. Comput. Harmon. Anal. 3 (1996) 1–9.
[2] C. Chauvière, J.S. Hesthaven, L. Lurati, Computational modeling of uncertainty in time-domain electromagnetics, SIAM J. Sci. Comput. 28 (2006) 751–775.
[3] C. Chen, J. Hong, L. Zhang, Preservation of physical properties of stochastic Maxwell equations with additive noise via stochastic multi-symplectic methods, J. Comput. Phys. 306 (2016) 500–519.
[4] W. Chen, X. Li, D. Liang, Energy-conserved splitting FDTD methods for Maxwell equations, Numer. Math. 108 (2008) 445–485.
[5] W. Chen, X. Li, D. Liang, Energy-conserved splitting FDTD methods for Maxwell equations in three dimensions, SIAM J. Numer. Anal. 48 (2010) 1530–1554.
[6] D. Cohen, G. Dujardin, Energy-preserving integrators for stochastic Poisson systems, Commun. Math. Sci. 12 (2014) 1523–1539.
[7] I. Daubechies, Orthonormal bases of compactly supported wavelets, Commun. Pure Appl. Math. 41 (1998) 909–996.
[8] M. Francoeur, M. Mengüç, Role of fluctuational electrodynamics in near-field radiative heat transfer, J. Quant. Spectrosc. Radiat. Transf. 109 (2008) 280–293.
[9] E. Faou, T. Lelièvre, Conservative stochastic differential equations: mathematical and numerical analysis, Math. Comput. 78 (2009) 2047–2074.
[10] J. Hong, S. Zhai, J. Zhang, Discrete gradient approach to stochastic differential equations with a conserved quantity, SIAM J. Numer. Anal. 49 (2011) 2017–2038.
[11] J. Hong, L. Ji, L. Zhang, A stochastic multi-symplectic scheme for stochastic Maxwell equations with additive noise, J. Comput. Phys. 268 (2014) 255–268.
[12] S. Jiang, L. Wang, J. Hong, Stochastic multi-symplectic integrator for stochastic Hamiltonian nonlinear Schrödinger equation, Commun. Comput. Phys. 14 (2013) 393–411.
[13] L. Kurt, T. Schäfer, Propagation of ultra-short solitons in stochastic Maxwell equations, J. Math. Phys. 55 (2014) 011503.
[14] L. Kong, J. Hong, J. Zhang, Splitting multi-symplectic integrators for Maxwell equations, J. Comput. Phys. 229 (2010) 4259–4278.
[15] K.B. Liaskos, I.G. Stratis, A.N. Yannacopoulos, Stochastic integrodifferential equations in Hilbert spaces with applications in electromagnetics, J. Integral Equ. Appl. 22 (2010) 559–590.
[16] T. Misawa, Energy conservative stochastic difference scheme for stochastic Hamilton dynamical systems, Jpn. J. Ind. Appl. Math. 17 (2000) 119–128.
[17] G. Da Prato, J. Zabczyk, Stochastic Equations in Infinite Dimensions, Encyclopedia of Mathematics and Its Applications, vol. 44, Cambridge University Press, 1995.
[18] S.M. Rytov, Y.A. Kravtsov, V.I. Tatarskii, Principles of Statistical Radiophysics 3: Elements of Random Fields, Springer, 1987.
[19] H. Zhu, S. Song, Y. Chen, Multi-symplectic wavelet collocation method for Maxwell equations, Adv. Appl. Math. Mech. 3 (2011) 663–688.